EFFECT OF INTERLAYER TEMPERATURE CONTROL ON INTERLAYER STRENGTH FOR LARGE FORMAT ADDITIVE MANUFACTURING OF HIGH-PERFORMANCE THERMOPLASTICS

A. Ramírez de las Heras, S. Benou, T. Osinga
Royal Netherlands Aerospace Centre NLR
Voorsterweg 31, Marknesse, 8316 PR, The Netherlands
Ana.Ramirez.de.las.Heras@nlr.nl

T. Wang, P. Consul
LEAM Technologies GmbH
Claude-Dornier-Str. 1, Building 401, 82234, Weßling – Germany
Patrick.Consul@leam.tech

ABSTRACT

With the increase of printing dimensions inherent to Large Format Additive Manufacturing (LFAM), the main challenge of extrusion-based additive manufacturing processes is also magnified: achieving a high interlayer bond quality. Parts manufactured through this process typically exhibit 50–75% lower mechanical performance in the Z-direction (across layers) with respect to X- and Y-directions. The impact of interlayer temperature control on the interlayer strength of a semi-crystalline polymer printed using LFAM has been evaluated. By using assisted heating during printing, the substrate temperature can be raised to the optimal processing range, allowing for the creation of high-quality bonds between the consecutive layers.

In this study, multiple sets of specimens are printed at different interlayer temperatures using neat and carbon fibre reinforced LMPAEK™ material. The interlayer bond strength is evaluated through mechanical testing and microscopy analysis, and compared with in-line measurements of the interlayer temperature. The results of this research demonstrate that active heating enables higher quality interlayer bond compared to unassisted printing, reducing the anisotropy of 3D printed parts.

1. INTRODUCTION

Advances in polymer and composites extrusion-based additive manufacturing technologies have led to the development of Large Format Additive Manufacturing (LFAM). This technology enables larger prints and higher outputs than ever before, and it has been adopted already in various fields, such as the maritime or the construction industries. Due to the extensive range of materials that can be processed with this technology, also the aerospace industry is showing interest regarding the printing of high-performance carbon fibre reinforced thermoplastics. Currently demonstrated applications vary from prototyping to tooling manufacturing, while potential is identified to apply such technology for end parts as well. However, printing of high-performance thermoplastics presents numerous challenges due to their high glass transition and melting temperatures. As these translate into high processing temperatures, forming interlayer bonds of high quality is this process' primary hurdle.

1.1. LFAM of high-performance polymers

Similarly to any other extrusion-based AM technology, in the LFAM process the material is heated beyond melting, and consequently forced through a nozzle and deposited on a print bed. Once the material exits the nozzle, its temperature drops due to natural convection without a controlled heat input. This implies that environmental conditions will play an important role on the material's final state, i.e. degree of crystallinity on semi-crystalline polymers. While other extrusion-based technologies, like filament desktop printing, allow for setting specific environmental conditions by means of a heated chamber, the printing volumes targeted by LFAM do not permit such control in a standard printing configuration. In addition to the large print volume, a common LFAM print cell includes key elements of large dimensions, such as a robotic manipulator in which the extruder is mounted to facilitate its movement. Only when counting on specialized high temperature robots it would be possible to condition the print cell at sufficiently high temperatures. As a result, LFAM of high-performance polymers, which experience large temperature gradients due to high extrusion temperatures, is often limited in part size or in final part quality.

NLR works for several years on addressing this challenge and, in the context of the NXTGEN Hightech Program of The Netherlands, has upgraded its LFAM setup with a heated print bed and a substrate heating device. With the intention of evaluating these upgrades, the present work aims to demonstrate the effect that thermal control has on the mechanical strength of additively manufactured high performance thermoplastics.

1.2. NLR's equipment upgrades

When depositing high performance thermoplastics on a non-heated print bed, the temperature deltas can exceed 300 °C. The resulting thermal shock often leads to bad adhesion to the print surface and internal stresses building up within the initial layers, which leads to warping, cracking or other undesirable effects. When printing on a **heated print bed**, this thermal impact can be reduced significantly, lessening or eliminating the aforementioned issues [1]. Additionally, the heated print bed will heat its closest environment and, depending on the size of the printing cell, this effect will be noticeable through several layers.

Considering the target LFAM build height (generally around or over a meter), the heated bed has a limited effect on thermal gradients through the complete print. When the **interlayer temperature** is insufficient, the bond between consecutive layers will not be fully developed, leading to reduced strength or possible delamination and part failure caused by the internal stresses. Traditionally, the solution was limited to adjusting the printing speed to achieve a specific layer time. This will ensure that the cooling down period is sufficient for the material to gain consistency for supporting the consecutive layer, but still enable the interlayer bond. As a result, the print size is directly limited, as the extruder's characteristics will define the maximum extrusion speed possible for the specific material.

To solve this, NLR upgraded its setup with a **substrate heating device**, named DEMEX (Directed Energy Material Extrusion), developed by LEAM Technologies GmbH [2], shown in Figure 1. This device uses feedback from a series of infrared cameras to control the substrate temperatures. It does so by heating with the power output of LED lights, cooling with pressurized air or adjusting the printing speed. In the initial experiments with DEMEX, NLR has been able to print larger quality parts than was possible before with high performance

carbon fibre reinforced thermoplastics (5 times longer layer lengths), and now aims to explore new applications, such as overprinting of stiffening elements on existing composite panels.

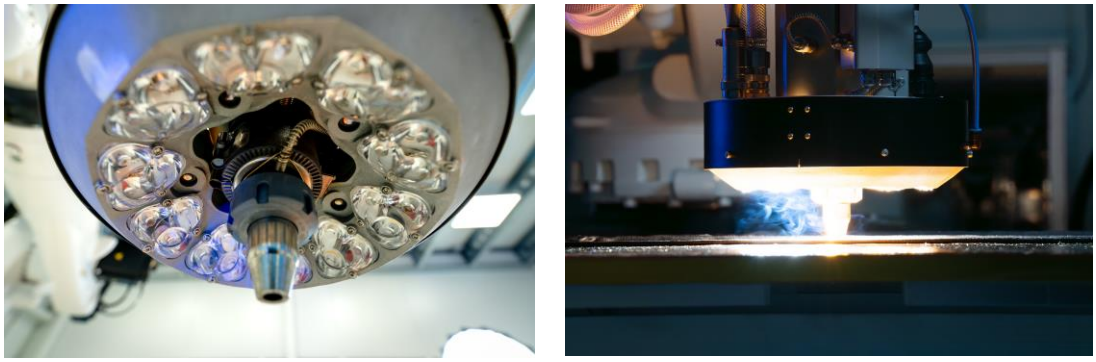

Figure 1. LEAM's DEMEX substrate heating device installed at NLR's LFAM setup

2. RESEARCH TESTS & EXPERIMENTS

In order to quantitatively evaluate the effect of Previous Layer Temperature (PLT) control on the interlayer mechanical strength, several cubes have been printed at different PLTs from which tensile specimens in printing (X) and stacking (Z) direction were extracted for testing.

2.1. Materials

Two versions of the same base polymer are used for this study: unreinforced LMPAEK™ Polymer 101 GRA and 30% carbon fibre reinforced LMPAEK™ Polymer 231 GRA (from now on identified as "unreinforced" and "reinforced", respectively). Testing the unreinforced version aims to verify the polymer's mechanical strength without the presence of porosity, often indicated to be (at least) partially promoted by the presence of fibres during the LFAM process [3]. Material's glass transition (midpoint), crystallization (peak) and melting (peak) temperatures are 153 °C, 264 °C and 305 °C, respectively. Prior to printing the materials were dried, and after printing all samples were annealed, following supplier recommendations.

2.2. Printing conditions

The printed specimens were manufactured using NLR's upgraded LFAM setup, consisting of a CEAD S25 extruder mounted on a KUKA robot, a heated print bed and an enclosed uncontrolled printing room of which temperature and humidity were tracked for each print. Printing speed was maintained constant, as well as print bed temperature and extrusion temperatures. Nozzle size and bead dimensions also remained the same for all cubes/materials. Per material, 4 cubes of 240 x 120 x 200 mm were printed, each one of them aiming at a different PLTs by using DEMEX. The tested setpoints are strategically selected just below, just above and well above melting temperature of the material. Based on literature, higher bond quality is expected to occur at PLTs above Tm [4]. Additionally, an uncontrolled cube is also printed and tested to understand the achievable material performance before equipment upgrades. All the printing parameters are shown in Table 1.

Table 1. Printing parameters

Parameter	Value
Previous layer temperature (target)	Uncontrolled; 300 °C; 320 °C; 340 °C; 360 °C
Extrusion temperatures (4 Heat Zones)	HZ1 = 330 °C; HZ2 = 345 °C; HZ3 = 365 °C; Nozzle = 365 °C
Print bed temperature	220 °C
Printing speed	24 mm/s
Nozzle	4 mm – flat
Bead dimensions (width x height)	6 x 2 mm

The DEMEX device was used to monitor the interlayer temperature in all cubes, and for PLT control in all cubes besides the un-controlled iteration. After printing, it is possible to extract for all robot positions during printing the temperature and applied LED power, as shown in Figure 2.

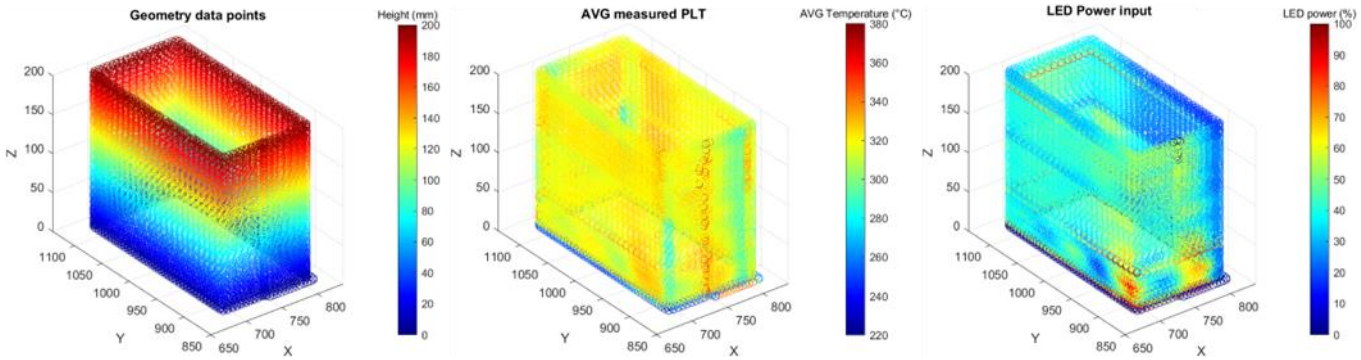

Figure 2. DEMEX data visualization – full print data points

For the data analysis, the regions of interest are filtered from the complete specimen dataset shown above, resulting in two data sets per iteration (each of the long sides of the printed cube), as shown in Figure 3. This is intended to remove possible misleading data points from the first layers (where the print bed can have an effect on the measurements), sharp corners (where the print area falls outside the measured field of view) and other possible deviations. Both average and mean values are calculated from the filtered data sets for PLT measurement and LED Power Input variables on each iteration. Standard deviation is also calculated.

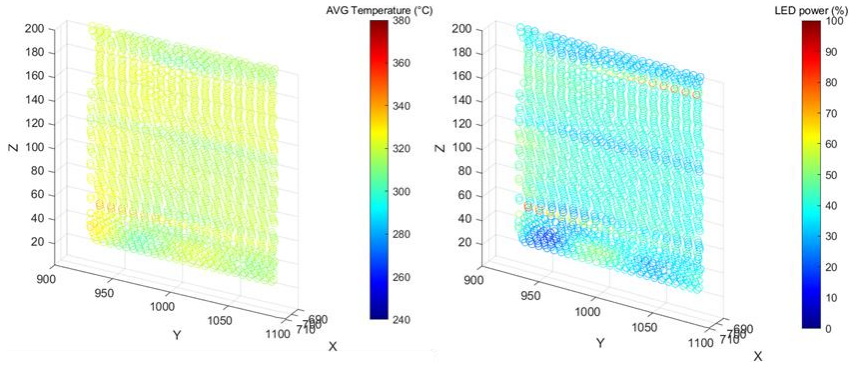

Figure 3. DEMEX data visualization - filtered data set (corresponding to one wall of one print)

2.3. Mechanical testing

After printing and annealing the cubes, a number of specimens are extracted from the long sides of each iteration. Prior to machining the tensile samples, both surfaces are milled flat until achieving the width specified by the test standard, but only after removing the bead edges to

eliminate notch effects (obtaining the effective bead width). From wall #1, tensile specimens in X-direction (printing direction) are obtained, while from wall #3, tensile specimens are oriented in Z-direction (across the layers). All samples correspond to Type I specimen as specified in the ASTM D638-14 standard, while tests are performed according to the same norm, with five specimens (plus one reserve) per cube /direction. In Figure 4 a visual definition of the testing directions and the considered effective bead width are shown.

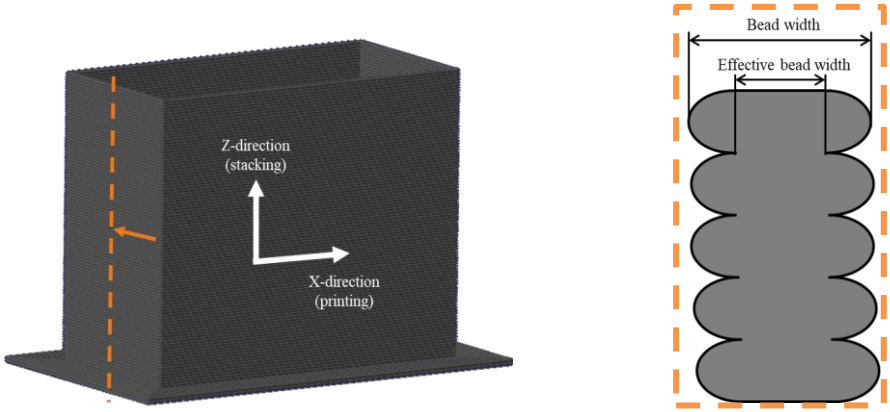

Figure 4. Definitions of testing orientation and considered effective bead width

3. RESULTS & DISCUSSION

In this section the results are discussed, evaluating the printing process, DEMEX measurements, mechanical testing and microscopic imaging results.

3.1 Printing outcome

During printing, a series of characteristics are evaluated for each cube: visual quality of the print, bead dimensional stability and signs of warping or other printing defects.

When printing the unreinforced polymer, warping issues were major and it was required to mechanically attach the print to the table. After printing the brim, it was held by means of metal strips and manual clamps (see Figure 5-left). The uncontrolled iteration for this material (where measured PLT was on average 270 °C) failed a few seconds after finishing printing, resulting in a large crack across several layers, therefore it hasn't been tested further (see Figure 5-right). From the next iteration (PLT = 300 °C) on, there were no issues found to print the unreinforced polymer.

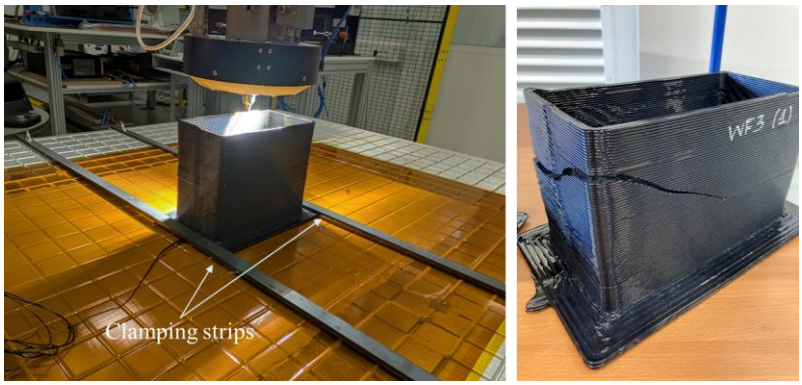

Figure 5.Unreinforced LMPAEK™ printing: (left) mechanical clamping to overcome extreme warping, and (right) failure after printing uncontrolled iteration

When printing the reinforced polymer, warping did not occur as the fibres increase the thermal conductivity and reduce the coefficient of thermal expansion (CTE) of the printed material, consequently reducing the thermal gradients throughout the part [5], [6]. In this case, all cubes were printed successfully. An overview of all the tested cubes is shown in Figure 6.

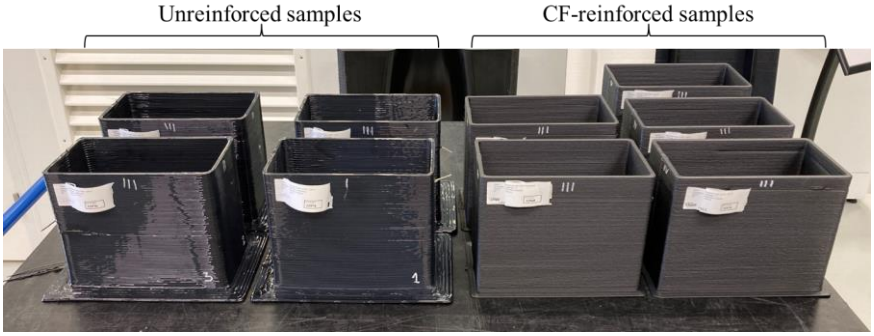

Figure 6. Overview of printed cubes

3.2 DEMEX measurements

Figure 7 shows LED power output for each intended PLT setpoint for the two different materials. For setpoints 300 °C and 320 °C, power output remained at around 30 and 40%, respectively. It is observed that the non-reinforced version requires slightly higher power to reach the 320 °C setpoint, likely due to the higher melting enthalpy of the unreinforced type, compared to the fibre reinforced version with 30% lower polymer content. When aiming for 340 °C, the power required was close to DEMEX's maximum capacity, while 360 °C setpoint exceeded the systems capabilities. The results from the specimens printed with PLT = 360 °C will not be further considered in this study.

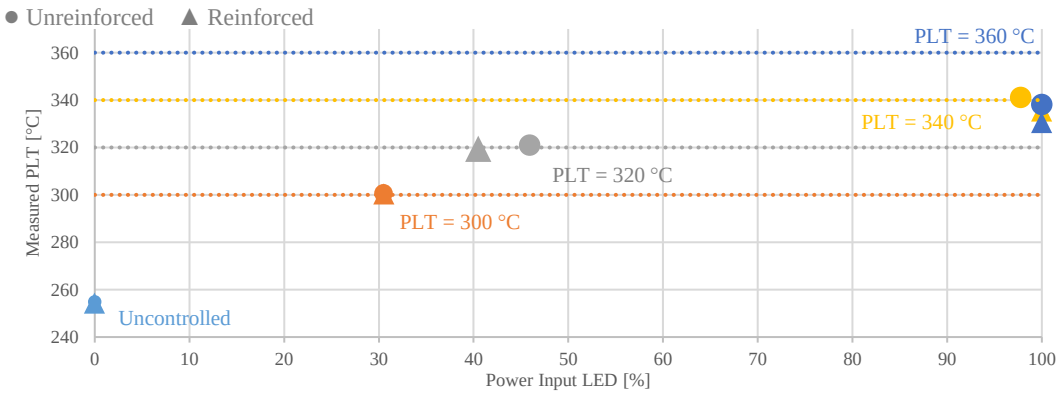

Figure 7. Power input required to achieve each intended setpoint vs actual PLT measurements

The observed temperature increase correlates well with the measured temperature increase for a single emitter module as tested under lab conditions on ABS (Acrylonitrile Butadiene Styrene) material, shown in Figure 8 for a comparable feed rate. In the used configuration, however, the power density in the heated spot should be twice as high with three emitters active at the same time achieving also double the temperature increase. The lower observed response could be due to a number of factors which will need further investigation. Possible causes are a higher specific heat capacity and density of LMPAEK™ compared to ABS, higher process temperatures leading to higher thermal losses, emitter malfunction, or misalignment of the optical lenses.

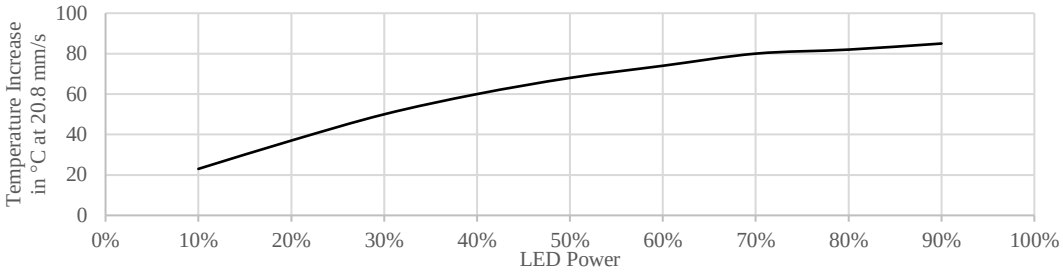

Figure 8. Temperature response for over LED power at 20.8 mm/s for a single emitter under lab conditions printing ABS

3.3 Mechanical testing results

Ultimate tensile strength values are represented for the unreinforced and reinforced materials in Figure 9 and Figure 10, respectively, for both testing directions. The results obtained for the unreinforced version show that active heating has little to no effect when testing in X direction. However, it is noteworthy that the obtained values are above the indicated in the material Technical Data Sheet, which correspond to injection molding specimens. On the other hand, in Z direction, an ultimate tensile strength increase of 457% is achieved from PLT = 300 °C to PLT = 340 °C. Presumably, this increase in performance would be even greater when compared to the unassisted cube that failed, where the recorded interlayer temperatures were on average 270 °C. This drastic improvement enables almost isotropic properties for this material when printed at PLT = 340 °C.

Similarly, the reinforced version shows only small differences in strength when testing in X direction. On the other hand, the performance improvement in Z direction was again noticeable, reaching an increase of 70% from uncontrolled to PLT = 340 °C.

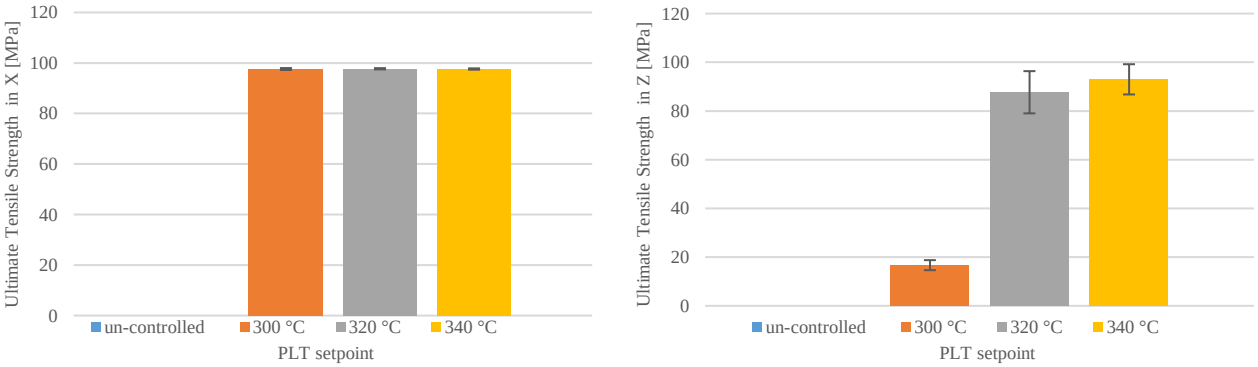

Figure 9. Ultimate Tensile Strength of the unreinforced version in (left) X and (right) Z direction

When analyzing the stress-strain curves (Figure 11), a clear difference is seen between the unreinforced and reinforced versions: the first presents ductile behavior while the second is brittle. For the same sample condition (X-direction and PLT = 340 °C) the unreinforced polymer reaches over 50% tensile strain at break, while the reinforced version stays well below the 2% threshold.

When analyzing the coupons tested in Z-direction, for the unreinforced version it is possible to observe the elongation and the final rupture crossing various layers. On the contrary, for the

reinforced version a clear straight separation occurs (presumably) between two consecutive layers without prior elongation (failure in the layer interface). In X-direction, and for both materials, the rupture is very similar, with a non-straight growth. A representative example for both testing directions is shown in Figure 12.

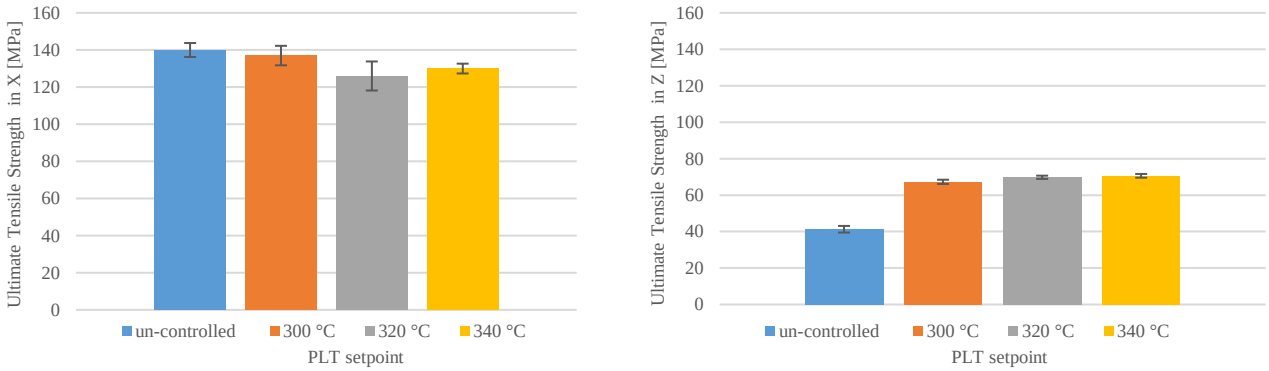

Figure 10. Ultimate Tensile Strength of the reinforced version in (left) X and (right) Z direction

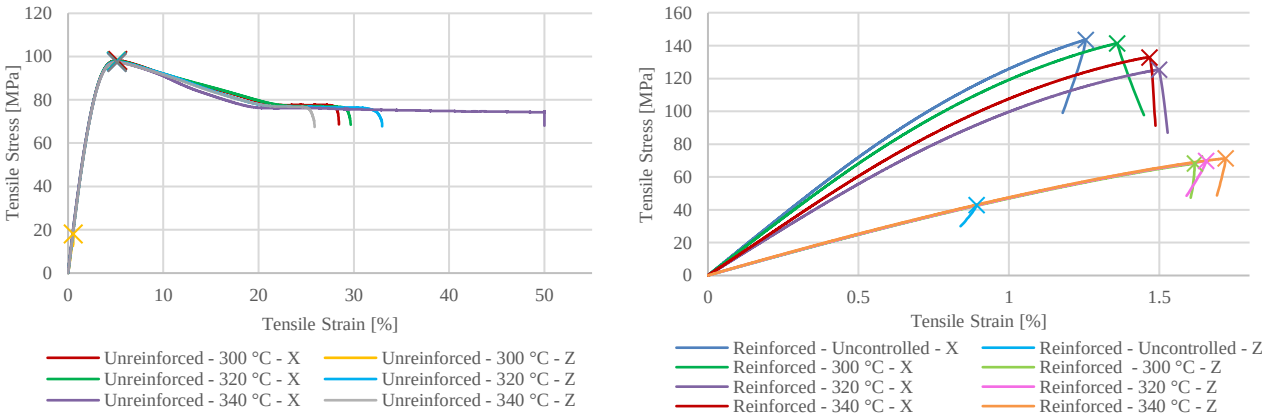

Figure 11. Stress-strain curves for (left) un-reinforced version and (right) reinforced version. Note: maximum tensile stress values are marked with an X for each curve

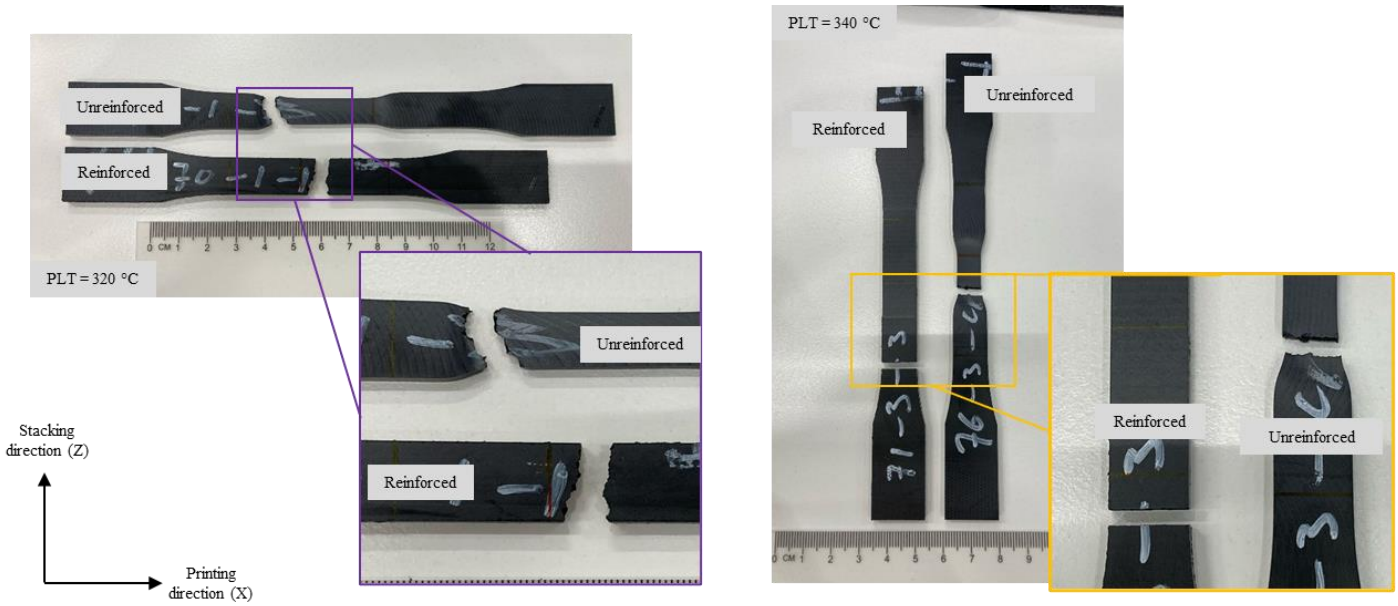

Figure 12. Visual differences in the failure of tensile specimens for both materials in both directions

3.4 Microscopy analysis

In order to understand the material appearance on a microscopic level, two types of images have been taken from each cube: (A) inspecting the plane perpendicular to the printing direction, and (B) at the plane following the printing direction. Samples type A were used to measure layer dimensions and effective width (where no significant variation was found between the samples), while images type B were used to analyze fibre distribution and alignment (in the case of the reinforced material), as well as porosity presence. In Figure 13, a visual representation of the extraction of the two samples is shown.

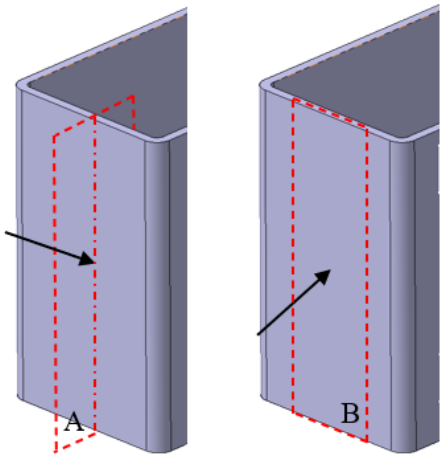

Figure 13. Schematic of microscopy samples

As expected (and demonstrated in the previous subsection), the presence of fibres clearly affects the material performance in the printing direction (X), increasing its ultimate tensile strength by 35% on average with respect to the neat polymer (see left graphs on Figure 9 & Figure 10). During printing, fibres adopt a certain level of orientation in the direction of movement, contributing to this increase in performance.

When observing samples taken from section type B for the reinforced material, it is possible to identify regions where fibres align in the printing direction (appearing horizontal in Figure 14-right), surrounded by regions with lower fibre alignment (appearing at an angle) and even some perpendicularly oriented (showing as quasi-circular shapes). The regions with high alignment are the interfaces between two layers, where shear forces during deposition are highest, causing wall effects and high fibre alignment. Inside the layer, fibres are possibly dragged by the rotational movement inside the extruder and randomly positioned in its final orientation, and with lower shear forces, fibres remain in this orientation during deposition. This was also observed by [7].

As can be inferred, when testing in the stacking direction, the matrix will be the element subjected to the load. This translates into a highly anisotropic behavior of the reinforced material (as seen in Figure 10).

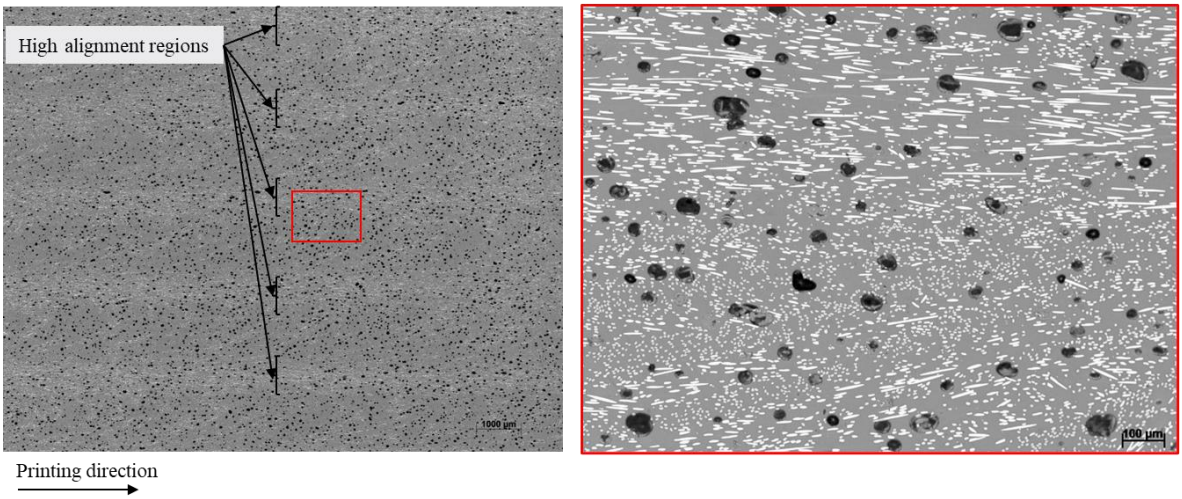

Figure 14. Fibre alignment across various layers. Overview (left) and detailed (right) microscopy images (type B) for reinforced sample with PLT = 340 °C

When comparing reinforced and unreinforced materials' microscopy images, besides the fibre presence there is another clear difference: the reinforced version exhibits a significant amount of porosity, whereas the unreinforced version is porosity-free (see Figure 15). Several hypotheses have been often discussed in literature when trying to identify the source of this porosity:

- Material conditioning: the release of moisture during the printing process would translate into porosity in the final part if the material has not been dried properly prior to the extrusion [8]. Both materials were dried according to recommendations, however, fibre reinforced and neat polymers will likely behave differently, therefore further investigation will be carried out to verify that material was dried properly.
- Introduction of air during the transport phase: it has been observed that, in general for this process, air is introduced in the extruder during the material transport from the dryer to the extruder. This generally occurs by means of pressurized air and, after this, if the air doesn't have an escape location along the extruder, it would remain in the material [9]. This wouldn't explain the difference between neat and fibre reinforced polymer – as they were printed with the same system – therefore it can be ruled out.
- Suboptimal printing parameters selection: printing temperature, speed or layer dimensions in relation to the nozzle size can have an effect on the formation of voids [10]. This remains of interest for further tests.
- Outgassing during the extrusion process: this could indicate that volatiles are released from the fibre sizing, which will be further investigated with the assistance of the material provider.

Further analysis of the unreinforced and reinforced samples didn't show any significant differences with the variation of interlayer temperature.

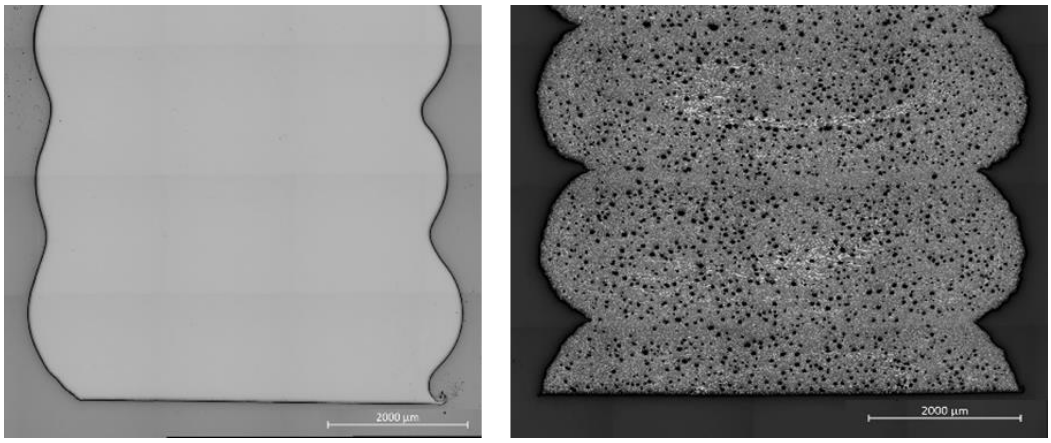

Figure 15. Examples of A type microscopy images for unreinforced (left) and reinforced (right) material versions

4. CONCLUSIONS

In the presented work, the effect of interlayer temperature on the final mechanical performance of 3D printed high-performance thermoplastics (neat and CF-reinforced) has been evaluated by means of tensile testing and complemented with microscopic imaging. From this, the following conclusions can be drawn up:

- By using the DEMEX system it was possible to raise the interlayer temperature up to 340 °C, where unassisted specimens reached around 265 °C on average. The achieved temperature is not reachable without active heating, i.e. reducing the layer time by increasing the printing speed, as the part would collapse due to insufficient hardening prior to the deposition of the next layer.
- In printing direction (X), material performance is barely influenced by interlayer temperature.
- In stacking direction (Z), material performance is heavily influenced by interlayer temperature. For the unreinforced material, from PLT = 300 °C to PLT = 340 °C an ultimate tensile strength increase of above 450% is observed. For the reinforced material, the increase from uncontrolled to PLT = 340 °C, is around 70%.
- It was possible to reach almost isotropic behavior in the unreinforced version for PLT = 340 °C.
- The presence of fibres played an important role on increasing mechanical performance in X direction (~35% higher in the reinforced version vs unreinforced). However, the appearance of porosity (only seen in the reinforced version, and possibly caused by the presence of fibres) acted to the detriment of material performance in Z direction. This translated in higher anisotropy for the reinforced material.

To summarise, increasing the interlayer temperature by actively heating with the DEMEX device has a significant (positive) effect on the interlayer strength. However, in order to exploit the full potential of this equipment upgrade, it is required to further investigate how to reduce the amount of porosity generated when printing fibre reinforced polymers.

- Acknowledgments

This project is made possible in part by a contribution from the National Growth Fund program NXTGEN HIGHTECH. For more information, visit www.nxtgenhightech.nl.

The authors would like to thank Victrex for the materials provided.

5. REFERENCES

[1] O. Bouzaglou, O. Golan, and N. Lachman, "Process Design and Parameters Interaction in Material Extrusion 3D Printing: A Review," *Polymers*, vol. 15, no. 10, Art. no. 10, Jan. 2023, doi: 10.3390/polym15102280.
[2] "LEAM - Demex." Accessed: Apr. 17, 2025. [Online]. Available: https://leam.tech/demex
[3] C. E. Duty *et al.*, "Structure and mechanical behavior of Big Area Additive Manufacturing (BAAM) materials," *Rapid Prototyping Journal*, vol. 23, no. 1, pp. 181–189, Jan. 2017, doi: 10.1108/RPJ-12-2015-0183.
[4] P. Consul, A. Chaplin, N. Tagscherer, S. Zaremba, and K. Drechsler, "Interlaminar strength in large-scale additive manufacturing of slow crystallizing polyaryletherketone carbon composites," *Polymer International*, vol. 70, no. 8, pp. 1099–1108, 2021, doi: 10.1002/pi.6168.
[5] L. J. Love *et al.*, "The importance of carbon fibre to polymer additive manufacturing," *J. Mater. Res.*, vol. 29, no. 17, pp. 1893–1898, Sep. 2014, doi: 10.1557/jmr.2014.212.
[6] N. Sayah and D. E. Smith, "Effect of Process Parameters on Void Distribution, Volume Fraction, and Sphericity within the Bead Microstructure of Large-Area Additive Manufacturing Polymer Composites," *Polymers*, vol. 14, no. 23, p. 5107, Nov. 2022, doi: 10.3390/polym14235107.
[7] N. Tagscherer, T. Schromm, and K. Drechsler, "Foundational Investigation on the Characterization of Porosity and Fibre Orientation Using XCT in Large-Scale Extrusion Additive Manufacturing," *Materials*, vol. 15, no. 6, p. 2290, Mar. 2022, doi: 10.3390/ma15062290.
[8] A. Hadi, A. Kadauw, and H. Zeidler, "The effect of printing temperature and moisture on tensile properties of 3D printed glass fibre reinforced nylon 6," *Materials Today: Proceedings*, vol. 91, pp. 48–55, Jan. 2023, doi: 10.1016/j.matpr.2023.04.641.
[9] F. Mattingly, V. Kumar, K. Chawla, W. Bras, V. Kunc, and C. Duty, "Vacuum-assisted extrusion to reduce internal porosity in large-format additive manufacturing," *Additive Manufacturing*, vol. 97, p. 104612, Jan. 2025, doi: 10.1016/j.addma.2024.104612.
[10] Y. Tao *et al.*, "A review on voids of 3D printed parts by fused filament fabrication," *Journal of Materials Research and Technology*, vol. 15, pp. 4860–4879, Nov. 2021, doi: 10.1016/j.jmrt.2021.10.108.